Unrolled MAPEM for SPECT reconstruction

Corentin Constanza[1], Théo Kaprelian[1], Ane Etxebeste[1], David Sarrut[1]

[1]INSA-Lyon, Université Claude Bernard Lyon 1, CNRS, Inserm, CREATIS UMR 5220, U1294, F-69373, Lyon, France

corentin.constanza@creatis.insa-lyon.fr

Objective

Investigate the use of an unrolled algorithm for SPECT reconstruction to enhance RPT dose quantification.

Introduction

- Single Photon Emission Computed Tomography (SPECT) can be used to plan and monitor treatment during Radiopharmaceutical Therapies (RPT) [1].
- Classical reconstruction methods such as MLEM/OSEM with Resolution Modeling (RM) suffer from noise and Gibbs Artifact [2].
- Alternatively, regularization techniques such as Relative Difference Prior (RDP) [3], necessitate a careful tuning of priors and parameters to prevent biased reconstruction.
- Finally, deep learning approaches, such as PVCNet-Sino [4], offer an alternative, though they typically suffer from limited interpretability as black-box models.

SPECT Reconstruction : MAPEM-OSL

- Reconstruct the image $x \in \mathbb{R}^N$ from $y \in \mathbb{R}^M$ the noisy measurement (i.e. the sinograms), knowing $A \in \mathbb{R}^{M \times N}$ the system matrix, can be seen as the following optimization problem:

$$x^* = \arg\min_{x>0} \mathcal{L}(x) + R(x) \tag{1}$$

where $R(x)$ is a regularization function and $\mathcal{L}(x)$ the negative loglikehood is defined as:

$$\mathcal{L}(x) = -\sum_{j=1}^{M} \left(y_i \log(\sum_{i \leq N} a_{ij} x_i) - \sum_{i \leq N} a_{ij} x_i \right) \tag{2}$$

- One can show that, to solve (1), we can use the *Maximum A Posteriori Expectation Maximization* with the "*one-step-late*" approximation (MAPEM-OSL) iterative scheme [5]:

$$x_{k+1} = \varphi(x_k, \theta_k) = \frac{x_k}{A^T(\mathbf{1}) + \nabla R_{\theta_k}(x_k)} A^T \left(\frac{y}{A x_k} \right) \tag{3}$$

- Our objective is to learn the gradient of the regularizer. To this end, we parameterize it as:

$$\nabla R_{\theta_k}(x) = \beta u_{\theta_k}(x) \tag{4}$$

Training strategie

- We unrolled the Equation 3 to learn the gradient of $R(x)$. For a Loss function L (ex: MSE), the gradient step is the following :

$$g^{unrolled}(\theta) = \partial_x L(\varphi^K(x_0, \theta))^\top \partial_\theta \varphi^K(x_0, \bullet)(\theta) \tag{5}$$

- Classical end-to-end unrolled learning strategies often require a compromise due to VRAM limitations: one must use either very small networks or very few unrolled iterations. To overcome this limitation, we propose using Jacobian-Free Backpropagation (JFB) [6, 7], which leads to the following update rule:

$$g^{JFU}(\theta) = \partial_x L(\varphi(\tilde{x}_{K-1}, \theta))^\top \partial_\theta \varphi(\tilde{x}_{K-1}, \bullet)(\theta) \tag{6}$$

- To stabilize training, we use gradient clipping and a warm-up strategy. Additionally, JFB contributes to improved stability, especially for larger numbers of iterations.

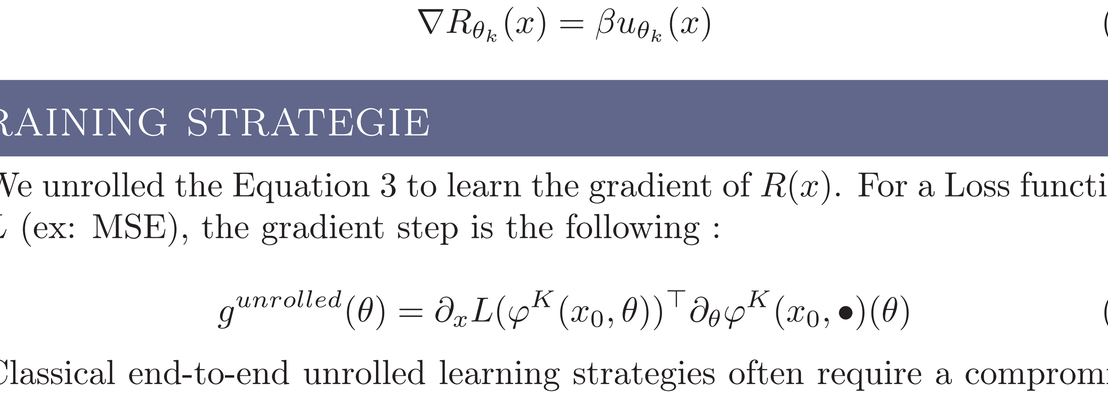

- The supervised training task lacks real-life ground truth, so we proposed to use a synthetic dataset, generated from segmented CT [4].

Results

	RM	RDP	PVCNet	U-MAPEM(6i)	JFU-MAPEM(18i)
PSNR$^\uparrow$	39.51	**42.15**	41.23	41.03	42.12
NRMSE$^\downarrow$	2.19	1.63	1.79	1.83	**1.62**
NMAE$^\downarrow$	0.37	0.27	0.25	0.34	**0.24**

Table 1: Global quantitative metrics results on simulated patients.

	Volume Activity Accuracy (VAA)$^\uparrow$				
organ	RM	RDP	PVCNet	U-MAPEM (6i)	JFU-MAPEM(18it)
liver	0.18	0.30	0.25	0.26	**0.53**
spleen	0.11	0.19	0.20	0.16	**0.37**
bladder	0.09	**0.12**	0.06	0.07	0.11
kidney	0.09	0.12	0.18	0.21	**0.29**
lesions	0.02	0.02	**0.07**	0.04	0.05

Table 2: Volume Activity Accuracy (VAA) [8] results on simulated patients.

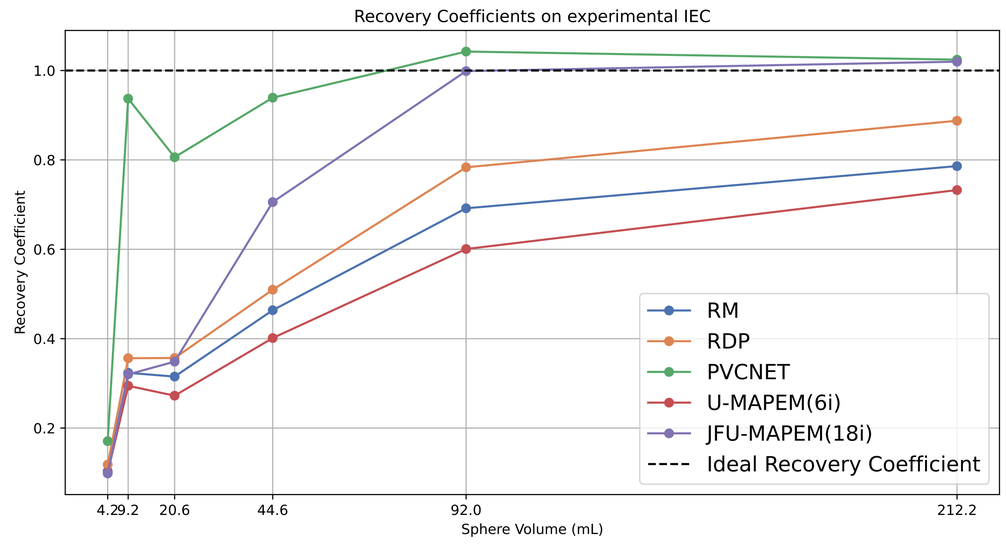

Figure 1: Recovery Coefficients (RCs) obtained on the 6-sphere IEC phantom experimental acquisition (177Lu, Siemens Intevo Bold).

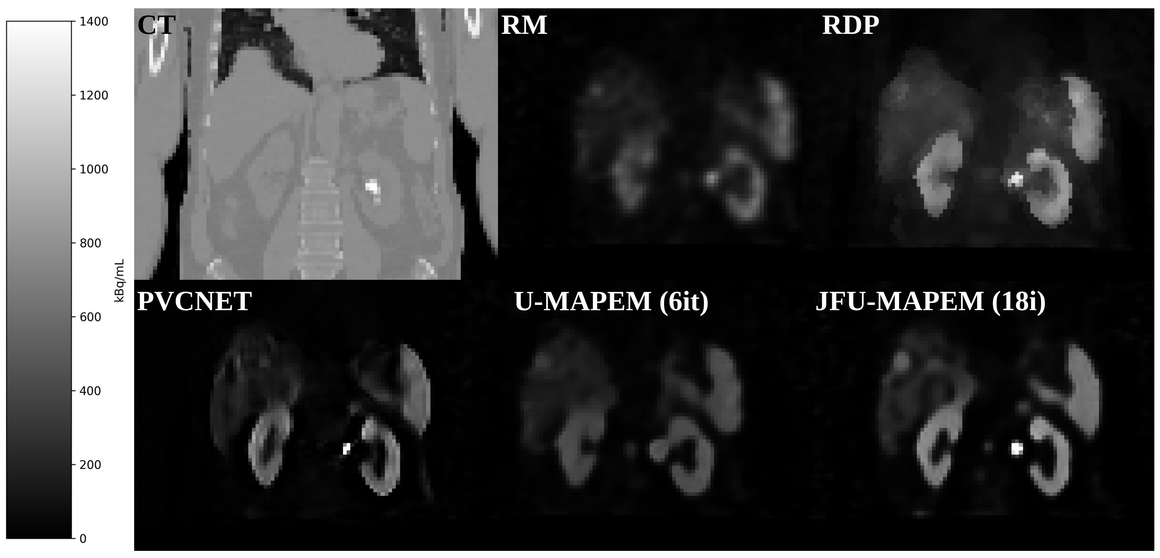

Figure 2: Exemple of Clinical reconstruction for a Lu-DOTATE RPT patient.

Conclusions

The proposed method demonstrates superior quantitative performance compared to traditional reconstruction techniques on both simulated and clinical data. These results further encourage the use of unrolled reconstruction methods for SPECT imaging quantification.

References

[1] Laure Vergnaud et al. In: *EJNMMI physics* 9.1 (2022), p. 37.
[2] Gengsheng L Zeng. In: *Journal of nuclear medicine technology* 39.3 (2011), pp. 213–219.
[3] Sangtae Ahn et al. In: *Physics in Medicine & Biology* 60.15 (2015), p. 5733.
[4] Théo Kaprélian et al. In: *2024 IEEE Medical Imaging Conference (MIC)* (2024), pp. 1–2.
[5] Peter J Green. In: *IEEE transactions on medical imaging* 9.1 (1990), pp. 84–93.
[6] Samy Wu Fung et al. In: *Proceedings of the AAAI Conference on Artificial Intelligence* 36.6 (2022), pp. 6648–6656.
[7] Leo Davy et al. In: *arXiv preprint arXiv:2506.13239* (2025).
[8] Julian Leube et al. In: *Journal of Nuclear Medicine* 65.6 (2024), pp. 980–987.